



PEARL

Radiological and elemental composition of cryoconite and glacier mice from Vatnajökull, Iceland

Smith, Emma; Clason, Caroline; Millward, Geoff; Taylor, Alex; Fyfe, Ralph

Published in:

Science of the Total Environment

DOI:

[10.1016/j.scitotenv.2024.175828](https://doi.org/10.1016/j.scitotenv.2024.175828)

Publication date:

2024

Document version:

Peer reviewed version

Link:

[Link to publication in PEARL](#)

Citation for published version (APA):

Smith, E., Clason, C., Millward, G., Taylor, A., & Fyfe, R. (2024). Radiological and elemental composition of cryoconite and glacier mice from Vatnajökull, Iceland. *Science of the Total Environment*, 951, Article 175828. <https://doi.org/10.1016/j.scitotenv.2024.175828>

All content in PEARL is protected by copyright law. Author manuscripts are made available in accordance with publisher policies. Wherever possible please cite the published version using the details provided on the item record or document. In the absence of an open licence (e.g. Creative Commons), permissions for further reuse of content should be sought from the publisher or author.

27 nearby proglacial sediments. In comparison to other glaciers in the Northern Hemisphere,
28 however, cryoconite from Icelandic glaciers contains some of the lowest activity
29 concentrations of key radionuclides. Consequently, cryoconite deposits that are released and
30 diluted during the melt and retreat of Icelandic glaciers are unlikely to be of environmental
31 concern following transport to proglacial areas.

32

33 **Keywords:** cryoconite; fallout radionuclides; metals; Iceland; glacier mice

34

35 **1. Introduction**

36 Cryoconite is a dark, granular solid that consists mainly of fine mineral particles (typically 60-
37 99%), with the remaining composition attributable to organic material and living
38 microorganisms (Cook et al, 2016; Clason et al., 2023a). Cryoconite has now been shown to
39 accumulate significant concentrations of fallout radionuclides (FRNs) and heavy metals across
40 mountain and polar regions globally (Rozwalak et al., 2022; Clason et al., 2023a), even in
41 remote, high latitude locations of the Southern Hemisphere (Buda et al., 2020; Owens et al.,
42 2023). In many sites FRNs have been detected in cryoconite with activity concentrations
43 elevated well above local soil and sediment backgrounds (Łokas *et al.*, 2016; 2017; 2018; 2019;
44 2022; Baccolo *et al.*, 2017; 2020a;b; Owens *et al.*, 2019; 2023; Clason et al., 2021). Mineral
45 particles found in cryoconite are mostly sourced from local substrates and wind-blown dust,
46 while organic matter is largely derived *in situ* from photosynthetic microbes that inhabit
47 glaciers (Zawierucha *et al.*, 2016). Furthermore, cyanobacteria play an important role in the
48 formation of cryoconite granules (Wejnerowski et al, 2023), since they produce extracellular
49 polymeric substances which have properties that contribute to the accumulation of dust and
50 micro-organisms. The chemical reactivity of cryoconite granules also leads to their
51 accumulation of FRNs, trace metals, metalloids, and nutrients such as phosphorus (Beard et

52 al., 2022; Clason et al., 2023a). Cryoconite is normally found either as a material dispersed on
53 the surface of glaciers or at the base of cryoconite holes in the ablation zone (Owens *et al.*,
54 2019; Baccolo *et al.*, 2020a;b). The dark colour of cryoconite also acts to reduce the albedo of
55 glacier surfaces, thereby contributing to enhanced melting of ice beneath the cryoconite layer,
56 promoting the formation of cryoconite holes and contributing to ice surface melting (Takeuchi,
57 2002).

58

59 Anthropogenic FRNs such as ^{137}Cs have been released into the global environment, mainly in
60 the Northern Hemisphere, since the second half of the 20th century (Łokas *et al.*, 2019) as a
61 result of atmospheric nuclear weapons testing, nuclear accidents, and the fragmentation of
62 satellites (Steinhauser et al., 2014). However, the presence of ^{241}Am in the environment is a
63 result of ^{241}Pu decay leading to increased ^{241}Am activity which is predicted to peak around
64 2100 (Baccolo *et al.*, 2020a). The presence of heavy metals in cryoconite results from their
65 increased deposition, by approximately tenfold, since the start of the industrial era (c.1850) as
66 a result of mining, industry, fuel burning, agriculture, transportation and waste disposal (Łokas
67 *et al.*, 2019). The atmosphere, oceanic currents, and rivers are regarded as significant transport
68 pathways for artificial radionuclides and heavy metals (Łokas *et al.*, 2019). Airborne FRNs,
69 possibly originating from the stratosphere (Corcho Alverado *et al.*, 2014), attach onto aerosols
70 or fine dusts (Wilflinger *et al.*, 2018), which are ultimately deposited on glacier surfaces.
71 Particulate fallout is aided by snowfall which effectively scavenges trace constituents from the
72 atmosphere (Singh et al., 2013). During the melt season water flows across the surface of
73 glaciers, particularly in the ablation zone where cryoconite is commonly found (Owens *et al.*,
74 2019). Hence, meltwater acts to mobilise and transport contaminants previously stored in the
75 snow and ice, which are accumulated in cryoconite deposits due to its chemically reactive
76 properties (Baccolo *et al.*, 2017; 2020a;b; Owens *et al.*, 2019).

77

78 Glaciers and ice sheets cover about 10% of Earth's surface, and act as an important source of
79 freshwater for downstream ecosystems and populations (Clason et al., 2023b). Understanding
80 the spatial variability of natural and anthropogenic contaminants in glaciated catchments is
81 important with respect to both the long-term health of the polar environment and for assessing
82 pressures on water quality. Cryoconite is one of the most radioactive of natural materials,
83 excluding those found in nuclear exclusion zones (Baccolo *et al.*, 2017). When glaciers melt
84 and retreat, cryoconite is released into the proglacial environment. Consequently, the raised
85 activity concentrations of FRNs found in cryoconite may act as a secondary source of
86 radioactive contaminants downstream (Owens *et al.*, 2019), with the potential for pollution of
87 local vegetation, aquatic habitats, and drinking water. Furthermore, the release of particulate
88 radionuclides from glaciers into downstream ecosystems could be taken up by biota, allowing
89 transfer within trophic chains causing contamination in higher species such as reindeer (Łokas
90 *et al.*, 2016; 2019). FRNs may also be taken up into other components of the supraglacial
91 ecosystem, such as 'glacier mice', little-studied ovate moss balls that are rich in microbial life,
92 contain a range of moss species, and have been observed to move across glacier surfaces in a
93 'herd-like' fashion (Coulson & Midgeley, 2012; Hotaling et al., 2020). It is thus important to
94 investigate the properties of materials in the transient supraglacial ecosystem to understand
95 whether the concentrations of the natural and anthropogenic contaminants it contains could
96 impact environments downstream. Although there are now numerous reports of the
97 concentrations of natural and anthropogenic contaminants in cryoconite from glaciers across
98 the globe (Rozwalak et al., 2022), Icelandic glaciers are a notable exception.

99

100 In this contribution we report the elemental compositions and activity concentrations of
101 radionuclides in cryoconite samples collected from the ice surfaces of Virkisjökull,

102 Skaftafellsjökull and Falljökull in Iceland. We also contribute new knowledge of the elemental
103 composition and activity concentrations of radionuclides in samples of glacier mice from
104 Falljökull, and explore the variability of natural and anthropogenic contaminants together with
105 the factors giving rise to their distribution.

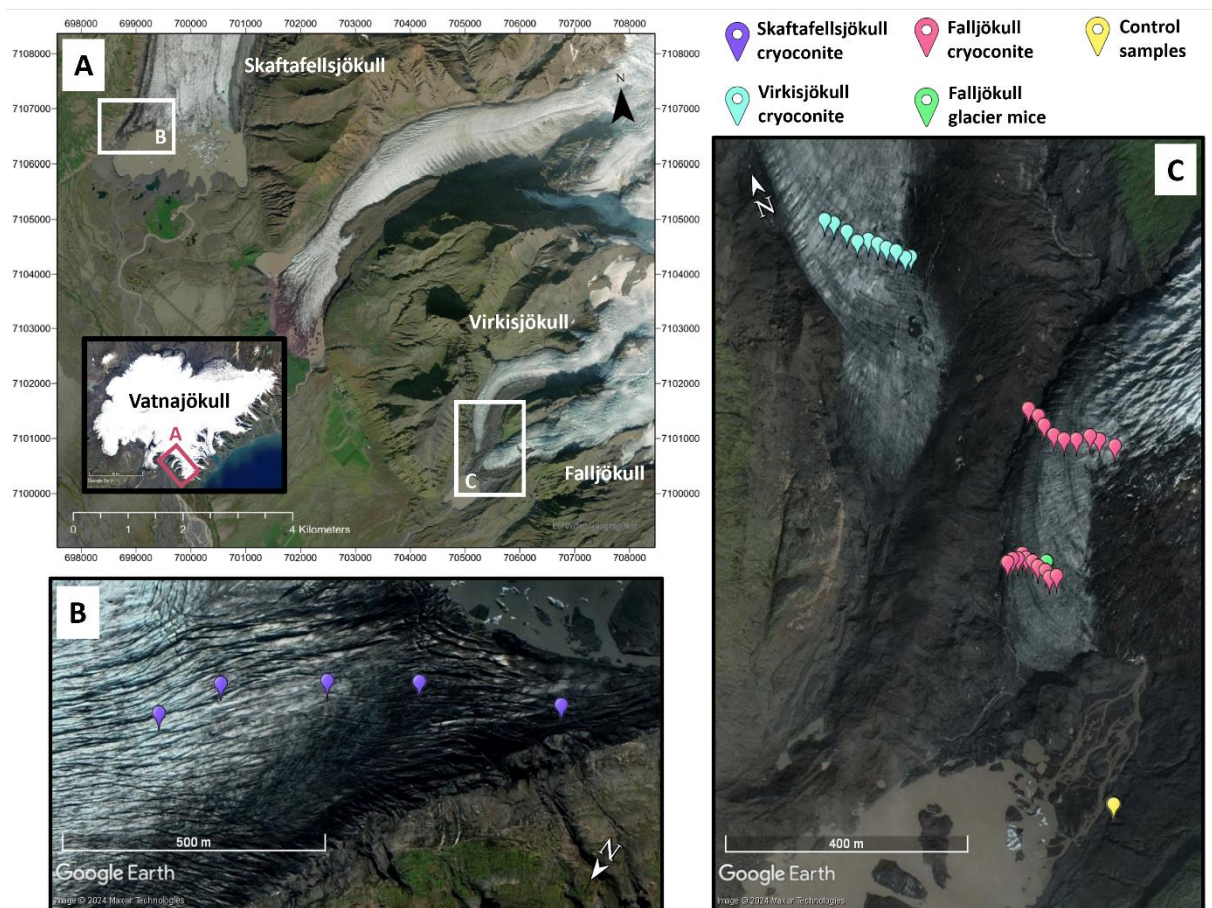
106

107 **2. Study area**

108 Virkisjökull, Skaftafellsjökull, and Falljökull are situated in south-east Iceland (Figure 1), and
109 are all outlet glaciers that descend from the Vatnajökull ice cap (Everest *et al.*, 2017).
110 Virkisjökull and Falljökull flow southwest from their source at over 1500 m above sea level
111 (asl) down to ~150 m asl. They are considered twin valley glaciers which separate around the
112 Rauðikambur nunatak at ~600 m asl (Phillips *et al.*, 2014; Everest *et al.*, 2017) before
113 reconnecting at ~210 m asl and terminating at ~130 m asl at a proglacial lake. Skaftafellsjökull
114 descends south from the Vatnajökull ice cap (Vilmundardóttir *et al.*, 2014) and terminates at
115 ~120 m asl. All three are temperate glaciers, and in recent decades have undergone a period of
116 rapid retreat in response to warmer summers and milder winters (Phillips *et al.*, 2014; Evans *et*
117 *al.*, 2017). Approximately 60% of Iceland's glaciers overlay active volcanoes, for example
118 there are seven volcanoes located under the Vatnajökull ice cap (Benediktsson *et al.*, 2024),
119 with Grímsvötn, Katla, and Öräfajökull notably having deposited tephra over Skaftafellsjökull
120 and nearby areas (Vilmundardóttir *et al.*, 2014). The proglacial regions of Iceland's glaciers
121 are typified by significant *sandur* such as Skeiðarársandur to the south of Vatnajökull (Arnalds
122 *et al.*, 2016), and Iceland experiences up to 135 days of dust storms annually. The area north
123 of Vatnajökull experiences desert-like conditions, while the ice cap can have up to 4000 mm
124 of precipitation annually (Einarsson, 1984). The predominant wind direction is from the east,
125 and the geology consists mainly of igneous basaltic rocks (Vilmundardóttir *et al.*, 2014).

126

127 The sea surrounding Iceland is one of the least polluted ocean areas of the world (Ministry of
 128 Environment, Iceland, 2006). The low contamination status is a result of its remote
 129 geographical location, its small population, and a relatively low number of industries releasing
 130 insignificant quantities of contaminants into the aquatic environment. The main industrial
 131 sources of pollutants are the shipyards, a tannery, a zinc-chrome coating plant, and aluminium
 132 and ferrosilicon plants (Ministry of Environment, Iceland, 2006). Contamination from heavy
 133 metals, radionuclides and other pollutants is thus largely transported from sources beyond
 134 Iceland.
 135



136
 137 **Figure 1.** (a) Study site including the position of outlet glaciers on the Vatnajökull ice cap; (b)
 138 cryoconite sampling locations on Skaftafellsjökull (purple); (c) cryoconite sampling locations on
 139 Virkisjökull (blue), cryoconite (pink) and glacier mice (green) sampling locations on Falljökull, and
 140 locations of the control samples (yellow).

141

142 **3. Methods**

143 *3.1 Sample collection and preparation*

144 A total of 10 cryoconite samples were retrieved from the surface of Virkisjökull, 5 from
145 Skaftafellsjökull, and 19 from Falljökull (Fig. 1) in July 2018, to characterise intra- and inter-
146 glacier variability in elemental composition and FRN content. Three control samples
147 (proglacial sediment) were also collected from an off-ice site in the Virkisjökull-Falljökull
148 forefield. Control samples were selected to provide a comparison of typical geochemistry
149 within sediments disconnected from glacial meltwater drainage pathways. Cryoconite samples
150 were collected from the ice surface or from within water-filled cryoconite holes using a plastic
151 pipette or a small plastic spatula, and control samples collected using a plastic trowel. Samples
152 were stored in water-tight containers for transportation to the Consolidated Radioisotope
153 Facility (CORIF) at the University of Plymouth, UK where they were freeze dried prior to
154 geochemical and radiological analysis. Moss balls (glacier mice) were also present in
155 abundance on the surface of Falljökull, and three were collected and preserved in bulk. On
156 arrival at CORIF the cryoconite samples were prepared immediately for radiological analysis
157 in order to capture the short-lived isotope ^7Be ($t_{1/2} = 54$ days). The cryoconite samples were
158 sieved, using a plastic mesh designed to isolate the $<63\mu\text{m}$ fraction. The cryoconite solids and
159 moss ball samples were freeze-dried for 48 h. Dried cryoconite samples were powdered by
160 hand using a mortar and pestle. Loose particulate matter in the strands of the moss balls was
161 shaken out and disaggregated using a plastic knife for subsequent counting. The prepared
162 samples were stored in acid-cleaned plastic bags in a refrigerator held at -30°C .

163

164 *3.2 X-Ray Fluorescence (XRF) spectrometry*

165 The geochemical compositions of the cryoconite and control samples were analysed by XRF
166 as loose powders which were packed into 40 mm diameter cups fitted with a 6 µm
167 polypropylene spectromembrane (Chemplex, USA). All samples were packed to the same
168 volume and left to settle for 24 hours prior to analysis. Analyses were undertaken by
169 wavelength-dispersive X-Ray fluorescence (WD XRF) spectrometry (Axios Max,
170 PANalytical, Netherlands). The instrument was operated at 4 kW using a Rh target X-ray tube.
171 During sequential analysis of elements tube settings ranged from 25 kV, 160 mA for low
172 atomic weight elements up to 60 kV, 66 mA for higher atomic weight elements. All analyses
173 were undertaken using the Omnia analysis application (PANalytical, Netherlands) under He
174 gas. Repeatability of the approach was assessed by repacking and analysing cryoconite samples
175 in triplicate with relative standard deviation found to be <10% across triplicates. This analytical
176 procedure has been validated by Clason et al. (2021) whereby an inter-comparison of results
177 obtained from a calibrated ICP-OES procedure which showed that XRF-Derived
178 concentrations were in close agreement, within 15% relative to ICP-OES for the elements of
179 interest.

180

181 *3.3 Gamma spectrometry*

182 The freeze-dried cryoconite samples were packed and sealed in gas tight plastic vials of 4 ml
183 volume containing up to 7 g of particulate sample. The prepared moss ball samples were packed
184 into aluminium boxes each holding approximately 25 g of solid phase. All samples were
185 incubated for 21 days to allow establishment of radioactive equilibrium between constituents
186 of the ²³⁸U decay scheme. Subsequently, activity concentrations of the target radionuclides
187 were determined using a well High Purity Germanium (HPGe) gamma spectrometer (EG&G
188 Ortec GWL-170-15-S) built with an ultra-low background specification, particularly for ²¹⁰Pb
189 detection. The gamma spectrometer was calibrated using a low-background soil spiked with a

190 certified mixed radioactive standard containing 12 radionuclides covering the gamma energy
191 range 46 to 1850 keV (#80717-669 supplied by Eckert & Ziegler Analytics, Georgia, USA).
192 All calibration relationships were derived using EG&G GammaVision software. All samples
193 were counted for a minimum of 24h. Total ^{210}Pb was measured by its gamma emissions at 46.5
194 keV and its unsupported component calculated by the subtraction of the ^{226}Ra activity, which
195 in turn was measured by the gamma emissions of ^{214}Pb at 295 and 352 keV, ^{137}Cs was
196 determined by its gamma emissions at 662 keV and ^{241}Am by the line at 59.4 keV. The stability
197 of the instrument was verified by undertaking regular quality control analyses of reference
198 materials, namely moss soil IAEA-2009-03, soil IAEA-TEL-2012-03, and spruce needles
199 IAEA-TEL-2016-03 (IAEA, Vienna, Austria) (Table A1). All activity concentrations were
200 decay corrected to the date of sampling and uncertainties were derived from counting statistics
201 and reported at ± 2 *sigma*.

202

203 Loss on ignition (LOI) for each sample was conducted by estimating the loss in weight
204 following the heating of accurately weighed samples contained in porcelain crucibles to 600°C
205 for 6 hours, following the procedure adopted by Łokas et al. (2022).

206

207 *3.4 Calculation of Enrichment Factors*

208 To emphasise the differences in the elemental concentrations from the various sample sites,
209 concentrations for both cryoconite and the control samples were normalised in terms of the
210 Enrichment Factor (EF), defined as:

$$211 \quad EF = \frac{\frac{M_m}{Al_m}}{\frac{M_S}{Al_S}} \quad (1)$$

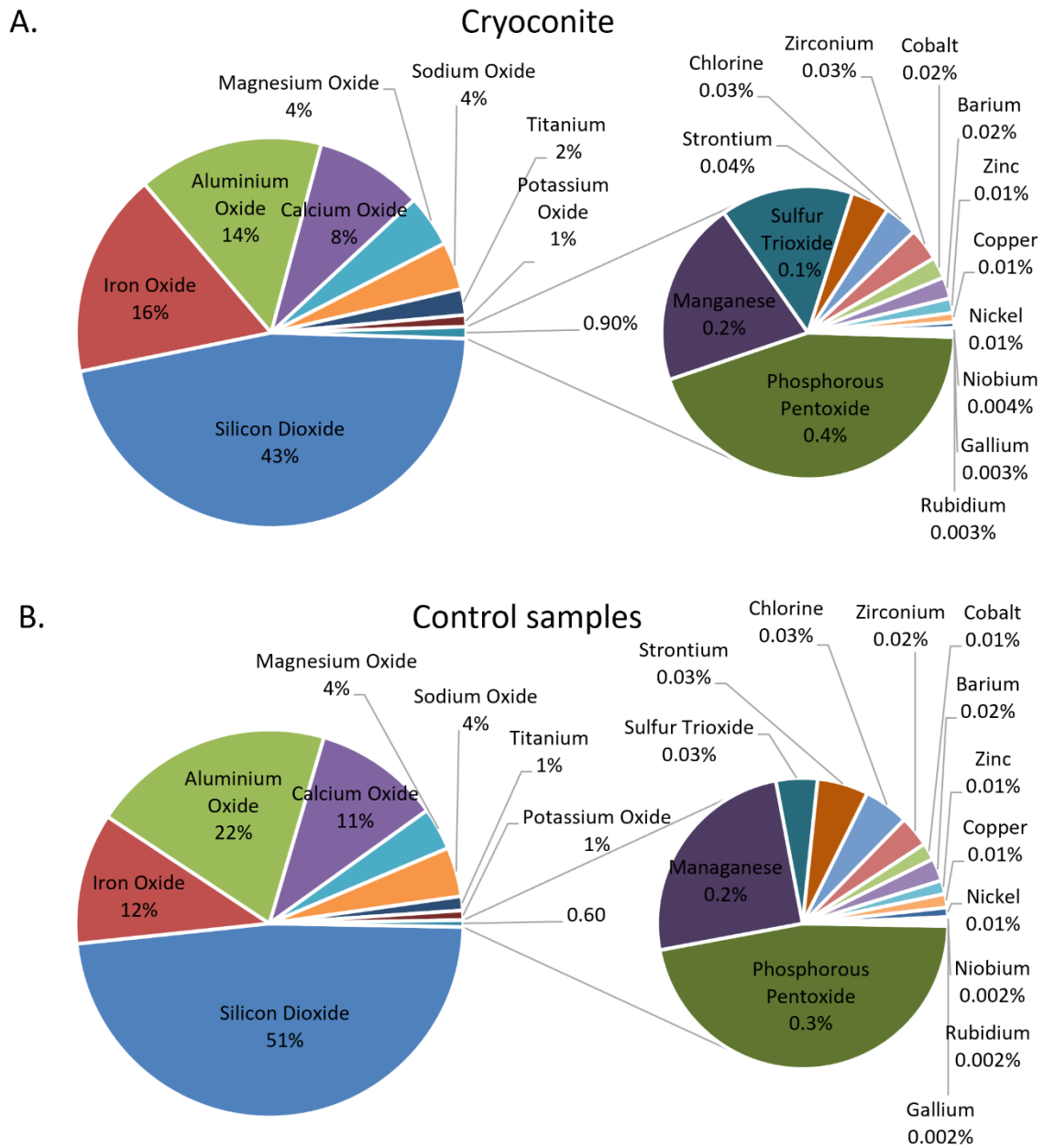
212 where M_m and Al_m are the measured metal and Al concentrations in cryoconite samples,
213 respectively, and M_s and Al_s are the metal and Al concentrations applicable to the composition
214 of the upper continental crust (Rudnick & Gao, 2014). $1 < EF < 3$ specifies minor enrichment,
215 $3 < EF < 5$ specifies moderate enrichment, $5 < EF < 10$ specifies moderate to severe enrichment,
216 and $EF > 10$ is classed as severe enrichment.

217

218 **4. Results**

219 *4.1 Inorganic composition of Icelandic cryoconite*

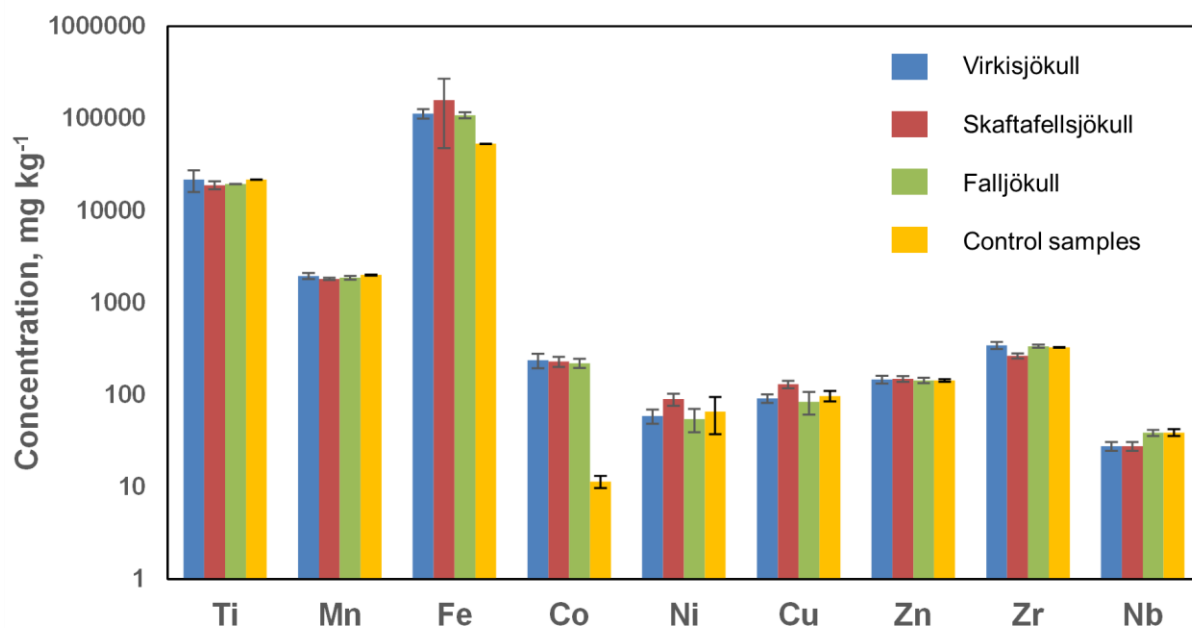
220 The analytical data is summarised as the mean percentages of the chemical composition of
221 cryoconite and the control samples (Figure 2). The sum of the concentrations from the XRF
222 spectrometric analyses adds up to ~93% as a result of other minor constituents in the sample
223 that were not determined. The mean concentrations of major constituents SiO_2 , Al_2O_3 and CaO
224 were higher in the control samples compared to the cryoconite samples (510,300; 215,300;
225 112,100 $mg\ kg^{-1}$ and 428,900; 142,400; 82,800 $mg\ kg^{-1}$ respectively), while cryoconite had
226 higher mean concentrations of Fe_2O_3 and P_2O_5 compared to the controls (156,900; 3995 $mg\ kg^{-1}$
227 ¹ and 116,300; 2826 $mg\ kg^{-1}$ respectively). For the minor constituents (Figure 3), cryoconite
228 from Virkisjökull had the highest concentrations of Ti (22,160 $mg\ kg^{-1}$), and Zr (340 $mg\ kg^{-1}$),
229 cryoconite from Skaftafellsjökull had the greatest concentrations of Ni, Zn and Cu (89; 149
230 and 129 $mg\ kg^{-1}$), and Falljökull cryoconite contained the highest concentrations of Nb (38 mg
231 kg^{-1}). Cryoconite from Virkisjökull and Falljökull contained similar concentrations of Cu and
232 Ni (92; 59 and 82; 55 $mg\ kg^{-1}$ respectively), which were both below the means for the control
233 samples (91 and 63 $mg\ kg^{-1}$). The mean concentration of Co in the control samples (171 mg
234 kg^{-1}) was notably lower than for cryoconite from Falljökull, Skaftafellsjökull and Virkisjökull
235 (218; 229 and 241 $mg\ kg^{-1}$ respectively).



236

237 **Figure 2.** a) Mean composition of cryoconite samples from Iceland; b) mean composition of control
 238 samples.

239



240

241 **Figure 3.** Concentrations of selected elements (mg kg⁻¹) determined in Icelandic cryoconite arranged
 242 in increasing atomic number: Virkisjökull (blue; n=10); Skaftafellsjökull (red; n=5); Falljökull (green;
 243 n=19); control samples (yellow; n=3).

244

245 The Enrichment Factor (EF) values for elements in cryoconite samples from Icelandic glaciers
 246 ranged from 1.3 to 5.3 – minor to moderate enrichment (Table 1). The highest EF values were
 247 found for Cu, followed by Ti and Ni, whereas lower EFs were obtained for Zn. Other elements,
 248 not shown, including Rb, Ba and Sr, had EFs<1. Similarly, control samples from ~280 m distal
 249 to the terminus of Falljökull had EF values that were similar to, or in some cases slightly greater
 250 than, the cryoconite values, especially for Ni and Cu. However, the enrichment of some metals
 251 in cryoconite from Iceland is significantly lower than the values for cryoconite from Sweden,
 252 as shown in Table 1 (Clason et al., 2021).

253

254

255 **Table 1.** Enrichment factors estimated using Eq. 1, based on the measured concentrations. The values
 256 for Icelandic cryoconite are compared to those obtained by Clason et al. (2021) for cryoconite from
 257 Sweden.

	Cr	Cu	Fe*	Ni	Pb	Ti	Zn
Concentration (mg kg ⁻¹) - Icelandic cryoconite	67±22	102±24	1.1x10 ⁵	67±19	29±19	20±1.5x10 ³	141±3
Enrichment Factors - Icelandic cryoconite	1.4±0.5	5.3±1.2	2.7±0.1	2.8±0.7	1.3±0.7	4.6±0.7	2.1±0.1
Enrichment Factors - Icelandic controls	1.7±0.2	6.4±2	1.3±0.0	3.4±0.2	ND	4.0±0.7	1.8±0.1
Enrichment Factors - Swedish cryoconite (Clason et al., 2021)	8.1 ± 0.9	15±5	3.2±0.3	9.2±1.3	17.1±4.4	3.2±0.1	4.0±0.5

258 *The full concentration value for Fe is $1.1 \times 10^5 \pm 0.015 \times 10^5$ mg kg⁻¹.

259

260 4.2 Radiological composition of Icelandic cryoconite

261 The cryoconite samples analysed here may be classed as having fine granules with a dark tone
 262 (Rozwalak et al., 2022; Figure A1). Total activity concentrations of radionuclides (Bq kg⁻¹) in
 263 cryoconite samples were highly variable (Figs. 4 and 5). The Virkisjökull samples had
 264 relatively low, close to background ¹³⁷Cs activity concentrations while the Skaftafellsjökull
 265 samples had significantly enhanced, but variable, ¹³⁷Cs activities (Figs. 4a; d). The activities of
 266 ¹³⁷Cs in the Falljökull samples had values intermediate to the other two sites (Figure 4g). The
 267 activity concentrations of excess ²¹⁰Pb (²¹⁰Pb_{ex}), where $^{210}\text{Pb}_{\text{ex}} = ^{210}\text{Pb}_{\text{total}} - ^{214}\text{Pb}$ (Figs 4b; e;
 268 h), were significantly higher than the ¹³⁷Cs activities where elevated values were obtained for
 269 the Skaftafellsjökull samples. Fewer samples had activities of ²⁴¹Am above the detection limit,
 270 with only ~50% of Falljökull samples having detectable ²⁴¹Am (Figure 4c; f; i). The maximum

271 activity concentrations for these radionuclides were coincident for some samples, for example
272 in sample 2 from Virkisjökull, sample 1 from Skaftafellsjökull and sample 5 from Falljökull.
273 This suggests that the activity concentrations of atmospheric fallout particulate matter were
274 well mixed prior to deposition. The solids collected from the control site (n=3) had significantly
275 lower activity concentrations for the key radionuclides compared to the cryoconite samples,
276 such that the mean activity concentration was $2.9 \pm 1.1 \text{ Bq kg}^{-1}$ for ^{137}Cs ; $<12.4 \pm 10.1 \text{ Bq kg}^{-1}$
277 for ^{210}Pb , whereas ^{214}Pb and ^{241}Am were below detection in all control samples.

278

279 The activity concentrations for ^7Be were highly variable, with relatively low values for
280 Skaftafellsjökull and marginally higher activities for Virkisjökull and Falljökull (Figure 5a; d;
281 g). The mean activities for ^{40}K in Falljökull and Virkisjökull were identical, statistically,
282 whereas the mean of the Skaftafellsjökull samples was only 1.1% lower (Figure 5b; e; h). The
283 mean LOI values for Virkisjökull, Skaftafellsjökull and Falljökull were $0.86 \pm 1.12\%$, $1.51 \pm$
284 0.60% and $0.96 \pm 0.20\%$, respectively (Figure 5c; f; i). These values are relatively low
285 compared to those found elsewhere (Łokas *et al.*, 2022; Clason *et al.*, 2023a).

286

287

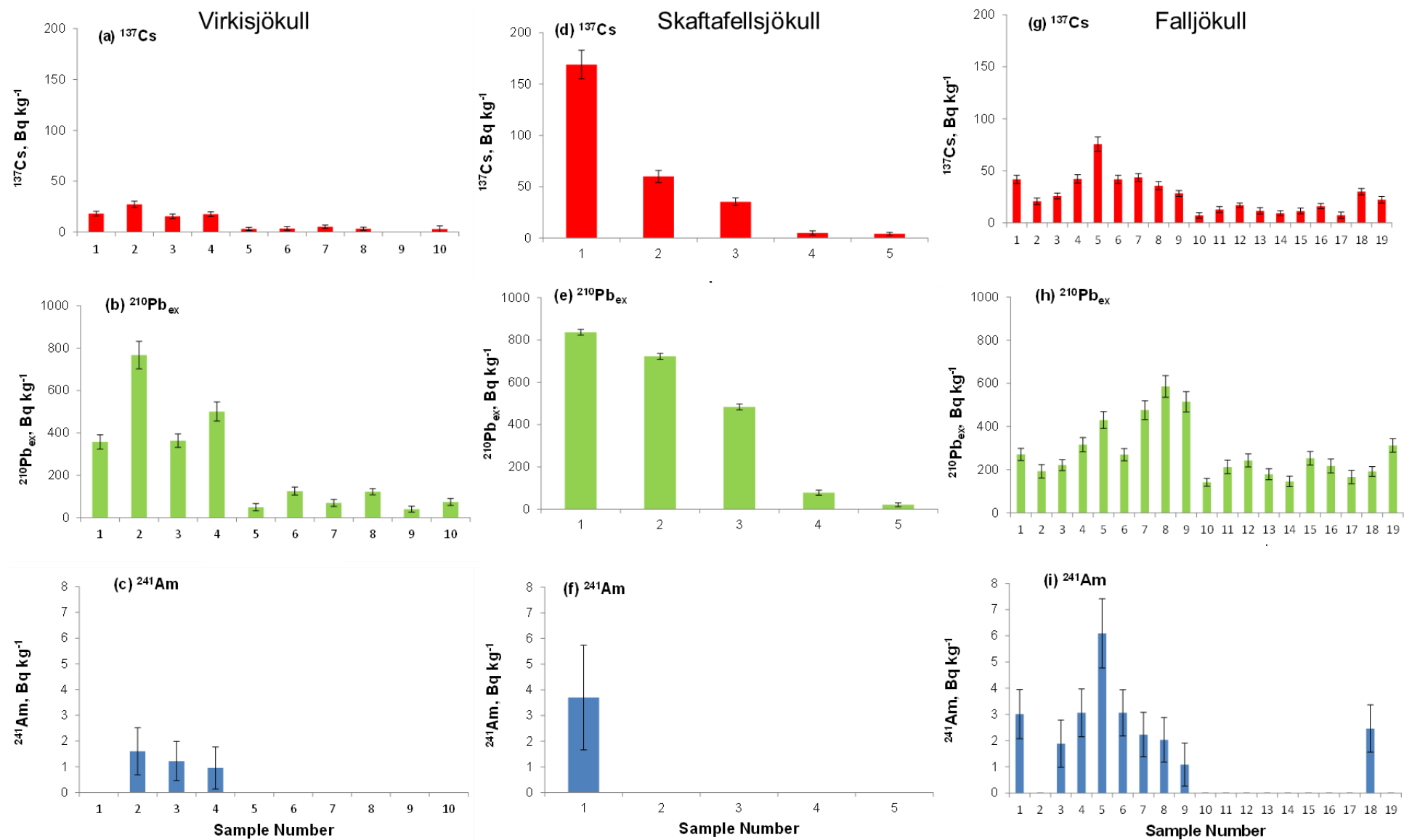


Figure 4. Activity concentrations (Bq kg⁻¹) and counting errors (±2σ) for ¹³⁷Cs (red), ²¹⁰Pb_{ex} (green) and ²⁴¹Am (blue) in cryconite samples from glaciers in Iceland: a, b, c - Virkisjökull; d, e, f - Skaftafellsjökull; g, h, I - Falljökull.

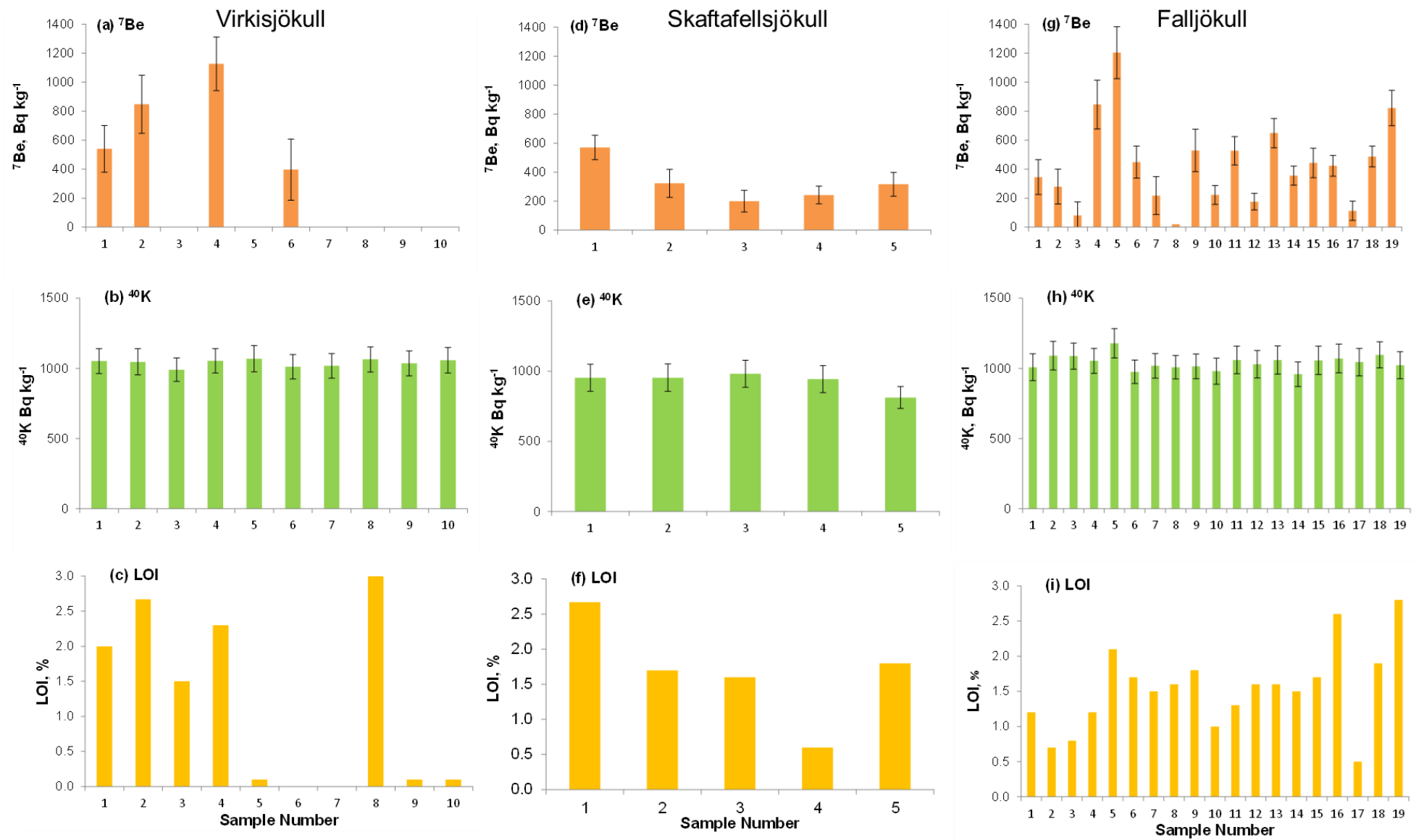
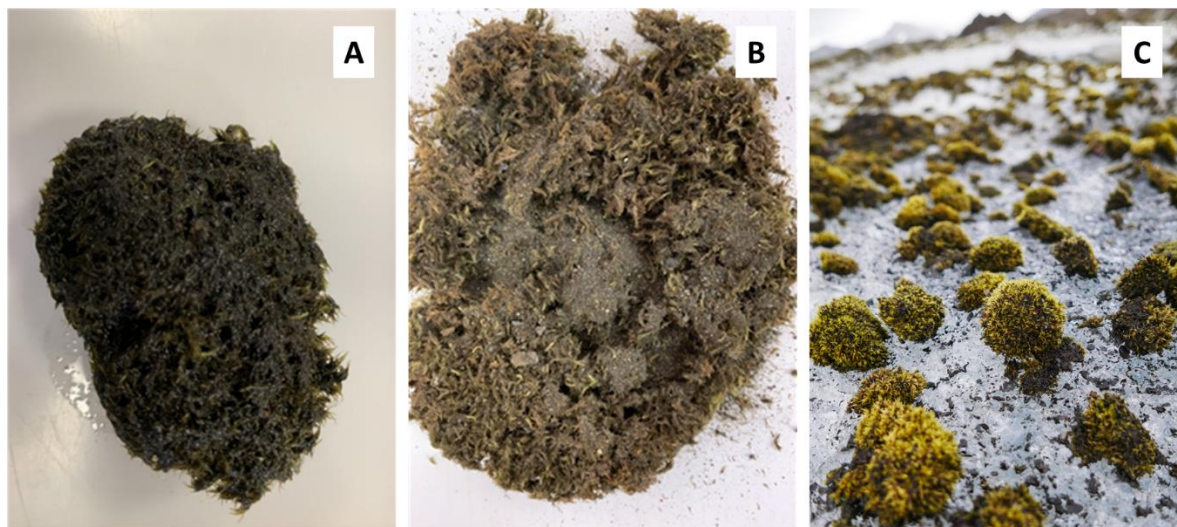


Figure 5. Activity concentrations (Bq kg $^{-1}$) and counting errors ($\pm 2\sigma$) for ${}^7\text{Be}$ (orange), ${}^{40}\text{K}$ (green) and LOI (yellow) in cryoconite samples from glaciers in Iceland: a, b, c - Virkisjökull; d, e, f - Skaftafellsjökull; g, h, i - Falljökull.

270 4.3 Radioactivity in glacier mice

271 Three samples of glacier mice (moss balls) were retrieved from the surface of Falljökull, an
272 example of which is shown in Figure 6a. The samples were dissected to allow access to their
273 interiors, which were filled with a solid phase similar to the cryoconite particles (Figure 6b).
274 Whole samples of glacier mice, and the internalised lithogenic material, were subjected to
275 gamma counting and XRF spectrometry as described above, and the results are shown in Table
276 2 and Figure 7. ^{137}Ca and $^{210}\text{Pb}_{\text{ex}}$ activities were higher in the whole moss balls than the
277 internalised dusts, and comparable to the activity concentrations reported for cryoconite in the
278 Falljökull-Virkisjökull glacier complex. ^{241}Am was below the minimum detectable activity for
279 all samples. Concentrations of selected elements are also comparable between glacier mice and
280 Icelandic cryoconite (c.f. Fig 3).

281



282

283 **Figure 6.** (a) an oblong glacier mouse as collected from Falljökull with any loose surface particulate
284 matter shaken out; (b) a cross section of a glacier mouse illustrating the lithogenic material (moss ball
285 dust) at the centre and the organic exterior (moss); (c) moss balls on the surface of Falljökull.

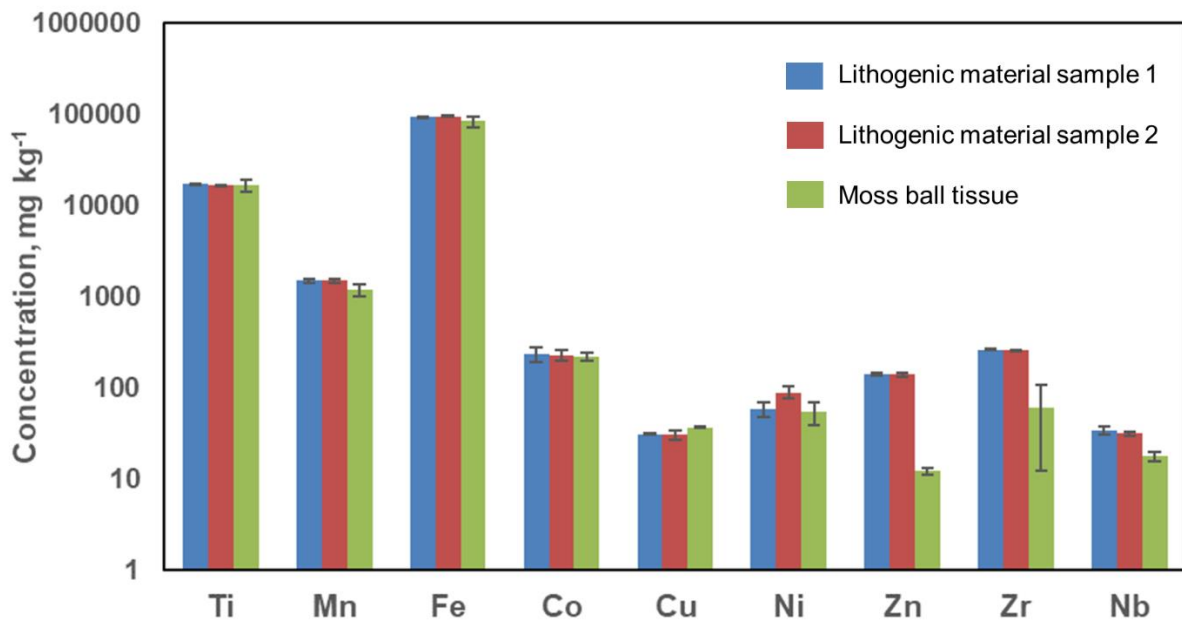
286

287

288 **Table 2.** Radionuclide activity concentrations (Bq kg⁻¹) in glacial moss balls and their dusts.

Sample	Shape	Total dry Weight, g	Activity Concentration, Bq kg ⁻¹			
			²¹⁰ Pb _{ex}	¹³⁷ Cs	²⁴¹ Am	⁴⁰ K
Moss Ball 1	Circular	44	638 ± 30	18.3 ± 0.9	MDA<2.4	681 ± 28
Moss Ball 2	Oblong	70	627 ± 28	17.1 ± 0.8	MDA<1.4	524 ± 21
Moss Ball 3	Oblong	52	672 ± 31	17.8 ± 0.9	MDA<1.9	631 ± 26
Moss Ball Dust 1	---	5.8	186 ± 36	8.9 ± 1.7	MDA<1.7	1067 ± 143
Moss Ball Dust 2	---	4.5	386 ± 5.3	15.1 ± 3.2	MDA<2.7	1486 ± 193
Moss Ball Dust 3	---	6.5	235 ± 4.5	10.6 ± 3.0	MDA<1.50	1035 ± 135

289



290

291 **Figure 7.** Concentrations of elements (mg kg⁻¹) determined in glacier mice from Falljökull (n=3)

292 arranged in increasing atomic number: lithogenic material sample 1 (blue); lithogenic material sample

293 2 (red); moss ball tissue (green).

294
295
296
297
298
299
300
301
302
303
304
305
306
307
308
309
310
311
312
313
314
315
316
317
318

5. Discussion

5.1 Natural and anthropogenic sources of contaminants in Icelandic cryoconite

The mean concentrations of SiO₂, Al₂O₃, CaO and K₂O in cryoconite, and the local control site, were lower than values for the upper continental crust (Rudnick and Goa, 2014). The major geochemical composition of cryoconite may thus be linked to the local geology and other natural local sources (Singh *et al.*, 2013). Volcanic ash samples comprised of mainly of basalt or andesite have been shown to contain relatively high SiO₂ contents (Table 3), whereas dust samples from near Skeiðarársandur and Mælifellssandur contain lower SiO₂ values and have other major element contents that cohere more closely with cryoconite samples analysed here. The elements Fe₂O₃, MgO and Na₂O are higher in volcanic ashes and dusts than the cryoconite samples, therefore natural sources may explain the higher concentrations. Minor elements in the cryoconite samples, Co, Ni, Cu, Zn, Zr and Nb, were found in higher concentrations than for both the upper continental crust values and those from the control site. The heavy metals found in the cryoconite samples may derive from industrial sources in Iceland discussed above, or from other, more distal sources by atmospheric transport (He *et al.*, 2023).

319 **Table 3.** Ranges of selected elemental compositions of volcanic ash from Grimsvötn and
 320 Eyjafjallajökull (Vogel et al., 2017) and dust samples from Skeiðarársandur and Mælifellsandur
 321 (Arnalds et al., 2016) compared to the mean cryoconite and control sample compositions from this
 322 study.

Element	Volcanic Ash^a,	Volcanic Dust^b,	Mean Icelandic	Controls^d,
	%	%	Cryoconite^c, %	%
SiO ₂	51.7-61.2	45.0-42.5	43.1 ± 1.8	51.3 ± 0.4
Al ₂ O ₃	13.6-14.7	14.5-14.2	14.4 ± 0.53	21.5 ± 0.4
Fe ₂ O ₃	14.8-9.2	16.1-18.9	15.8 ± 1.3	11.6 ± 0.02
MgO	5.83-2.13	6.2-4.9	4.3 ± 0.5	3.8 ± 0.09
CaO	9.54-4.92	12.0-11.6	8.5 ± 0.7	11.2 ± 0.3
Na ₂ O	3.01-5.26	4.0-4.1	3.6 ± 0.2	4.36 ± 0.2
K ₂ O	0.15-1.66	---	0.58 ± 0.08	0.084 ± 0.002
Ti	0.016-0.010	2.1-3.4	2.0 ± 0.4	0.12 ± 0.03

323 ^aVogel et al., 2017; ^bArnalds et al., 2016; ^cThis study (n=34); ^dThis study (n=3).

324

325 5.2. Radionuclides in Icelandic cryoconite

326 Nuclear weapons testing and nuclear accidents, including Chernobyl in 1986 and Fukushima
 327 in 2011, have led to contamination of regions across the Northern Hemisphere (Steinhauser *et*
 328 *al.*, 2014). For example, ¹³⁷Cs was introduced into the environment as early as 1945 and beyond
 329 during periods of nuclear weapons testing (UNSCEAR, 2000). The anticlockwise circulation
 330 of the atmosphere has allowed a global redistribution of 545 Mt of radioactive waste products
 331 generated by atmospheric testing and nuclear accidents through aerial transport. The potential
 332 for long-term fallout of waste from nuclear tests has been emphasised in research which shows
 333 that ¹³⁷Cs and Pu radionuclides can persist in the stratosphere for 2.5-5 years, and longer than
 334 previously estimated (Corcho Alvarado et al., 2014). However, Iceland received comparatively

335 less fallout from Chernobyl than other regions of the Northern Hemisphere, which is a likely
336 contributing factor to the lower activities of ^{137}Cs found in Icelandic cryoconite compared to
337 other areas such as central Europe and Scandinavia (Clason et al., 2023a). Strong spatial
338 differences in local surface topography, winds, and precipitation also contribute to the
339 considerable variability observed in the ^{137}Cs deposited in soils and vegetation across Iceland
340 by historical nuclear activities (Palsson et al., 2002). Furthermore, Iceland experiences up to
341 135 dust storms annually, which could potentially dilute atmospheric FRNs before being
342 deposited onto glacier surfaces, contributing to the relatively low activity concentrations in
343 cryoconite in this region. Vatnajökull is subject to frequent and strong katabatic winds and the
344 ensuing dust storms are highly effective at eroding and redistributing particulate matter
345 deposited on glacier surfaces, including dry cryoconite granules (Hannesdóttir et al., 2013).

346

347 Owens *et al* (2019) and Łokas *et al* (2022) have highlighted the importance of organic matter
348 in the accumulation of radionuclides due to its chemical complexation properties. Thus, the
349 variability in activity concentrations of radionuclides between cryoconite samples from Iceland
350 and other locations in the Northern Hemisphere may also be explained by the organic matter
351 content of the solids (Clason et al., 2023a). The cryoconite samples analysed here have a
352 relatively low organic content, in the range 0.0-2.9% (c.f. 0.0-38.5% for cryoconite from sites
353 globally; Clason et al., 2023), and a potential explanation for this is the influence of active
354 volcanoes in Iceland contributing to the deposition of volcanic ash onto glacier surfaces (Lutz
355 *et al.*, 2015). The prevalence of volcanic ash and dust influences the mineral content of
356 cryoconite while also providing various nutrients (Lutz *et al.*, 2015; Meinander *et al.*, 2016) to
357 the potential benefit of the microbial community in cryoconite (Nagatsuka *et al*, 2014). The
358 precise role of the glacier microbiome in accumulating contaminants, and how this will change
359 under future increased meltwater production, however, is yet to be explored in detail.

360

361 Icelandic cryoconite samples also contain ^7Be , a cosmogenic radionuclide that forms when
362 high energy cosmic radiation interacts with oxygen and nitrogen in the upper atmosphere. The
363 activities of ^7Be in the Icelandic samples may be a result of its geographical location in the
364 higher latitudes (Denk *et al.*, 2011), where a hole in the ozone layer over the Arctic could allow
365 the access of fallout of atmospheric ^7Be . Since ^7Be has a short half-life and the Icelandic
366 samples show relatively high activity concentrations, this indicates that ^7Be was deposited with
367 the cryoconite samples soon before sample collection. This is in line with the findings of
368 Baccolo *et al* (2020a) for cryoconite in the European Alps.

369

370 *5.3. Radionuclide activity in glacier mice*

371 Moss has often been used as a bioindicator of environmental pollution due to its ability to
372 accumulate atmospheric radionuclides (Baccolo *et al.*, 2020b). Moss balls or ‘glacier mice’ are
373 found on Icelandic glaciers and have also been described for a limited number of other glacier
374 sites around the world (Hotaling *et al.*, 2020), with glacier mice on Falljökull previously having
375 been shown to be a habitat for a range of invertebrate fauna (Coulson and Midgley, 2012).
376 Glacier mice have high organic matter content and can accumulate significant amounts of silt
377 by trapping fine dust, and also have a capacity to hold water, supporting a moist organic habitat
378 of importance to a range of invertebrates, including Collembola, Nematoda, and Tardigrada
379 (Coulson and Midgley, 2012). Our analyses of moss balls (n=3) gave a mean ^{137}Cs activity
380 concentration of $17.7 \pm 0.9 \text{ Bq kg}^{-1}$ (Table 2) which fits into to the range of 7.3-75.7 Bq kg^{-1}
381 for values of ^{137}Cs in the Falljökull cryoconite samples (Fig. 4g). Similarly, $^{210}\text{Pb}_{\text{ex}}$ in the moss
382 balls had a mean value of $646 \pm 23 \text{ Bq kg}^{-1}$ compared to a range of 142-586 Bq kg^{-1} for
383 Falljökull cryoconite (Fig. 4h). Consequently, the activity concentrations in whole glacier
384 mice, and in the internalised solid phase (Table 2), are similar to those found in cryoconite on

385 the same glacier. Koltonik et al. (2024) collected samples of glaciers mice from
386 Austerdalsbreen in Norway in 2021, reporting a median of 177 Bq kg⁻¹ for ¹³⁷Cs and 974 Bq
387 kg⁻¹ for ²¹⁰Pb for moss balls sampled from the ice surface. While ²¹⁰Pb concentrations are
388 comparable to those reported here, ¹³⁷Cs is an order of magnitude higher in the Norwegian
389 samples, and in line with reported regional variability in anthropogenic FRN concentrations in
390 cryoconite (Clason et al., 2023). Further studies of the processes involved in the uptake of
391 radionuclides into glacier mice are required to improve understanding of contaminant
392 acquisition mechanisms.

393

394 *5.4 Impact on the downstream environment*

395 The impact of heavy metals on organisms, including humans, depends on their mobility in the
396 environment, the chemical species, and the dose taken up (Tchounwou *et al.*, 2012). Some
397 heavy metals are essential micronutrients for humans and animals but can also be harmful in
398 excess quantities (Dietz *et al.*, 1998). Heavy metals of concern in Icelandic cryoconite include
399 Co, Cu, Ni, Zn (Emsley, 2001). Canadian Sediment Quality Guidelines (SQG) for Cu, Zn and
400 Ni are shown in Table 4 (CCME, 1995), and comparison against concentrations found in
401 cryoconite suggests that levels of these potentially toxic elements are not concerning. Nickel
402 is found in cryoconite at levels exceeding the probable effects level (PEL), however, the level
403 of Ni is lower in cryoconite when compared with the Norwegian Moderate values.

404

405

406

407

408

409

410 **Table 4.** Current Sediment Quality Guidelines (SQG) for Cr, Cu, Ni, Pb, and Zn (mg kg⁻¹) and
 411 comparison with the maximum levels found in Icelandic cryoconite samples. TEL = minimum adverse
 412 effects level; PEL = probable effects level; CB PEC = Consensus Based probable effect concentrations;
 413 and Norwegian Moderate.

Guideline Parameters,	Cr	Cu	Ni	Pb	Zn
mg kg⁻¹					
TEL	52.3	18.7	48	30.2	124
PEL	160	108	36	112	271
CB PEC	43.4	31.6	22.7	25.8	121
Norwegian Moderate	100	150	130	120	700
Maximum level in cryoconite	143 ¹	143 ¹	71.5 ¹	112 ¹	174 ²

414 ¹Sample from Skaftafellsjökull; ²Sample from Virkisjökull.

415

416 In terms of radioactivity, ¹³⁷Cs, ²¹⁰Pb, and ²⁴¹Am are the radionuclides of most concern when
 417 deposited into the environment where the biological damage caused by these radionuclides
 418 depends on the radioactive half-life (i.e. persistence and activity in the environment), the
 419 chemical form and mobility in the environment, route of exposure, and the type of radiation
 420 emitted during decay. Activity concentrations of ¹³⁷Cs, ²¹⁰Pb and ²⁴¹Am in cryoconite samples
 421 from Iceland are much lower than the activity concentrations measured on other glaciers in the
 422 Northern Hemisphere (Table 5), however they still exhibit higher activity concentrations of
 423 radionuclides compared to the off-ice control site. This highlights the ability of cryoconite to
 424 effectively accumulate radionuclides even in regions with lower levels of atmospheric
 425 contaminant deposition. Davidson et al. (2023) assessed the potential chemical lability of these
 426 radionuclides when subject to various chemical environments for cryoconite samples from
 427 Isfallsglaciären, Sweden (Clason *et al.*,2021) and Skaftafellsjökull, Iceland. A three-stage
 428 sequential chemical extraction comprising fractions of radionuclides that are (1) exchangeable,

429 (2) reducible, (3) oxidisable and (4) residual was used to assess the radionuclide accessibility.
430 ^{137}Cs was strongly bound to the cryoconite matrix resulting in <20% removal after three
431 extraction steps. In contrast, $^{210}\text{Pb}_{\text{ex}}$ and ^{241}Am were more chemically mobile and ~90% and
432 70% respectively were removed by stage 3. These releases indicate the chemical mobility of
433 radionuclides in cryoconite, and hence their potential for human, animal and environmental
434 impact in glacial environments.

435

436 Overall, it is unlikely that the activity concentrations, and contaminant concentrations, we
437 present for cryoconite and glacier mice in Iceland will have serious consequences for life in
438 the downstream environment. It has previously been shown in a study of Castle Creek glacier
439 in Canada (Owens *et al.*, 2019) that clastic materials in the proglacial zone exposed following
440 recent glacier retreat and sediments from a proglacial stream did not contain high levels of
441 radioactive or stable contaminants in comparison to cryoconite at this site. This is likely a result
442 of the dilution effect from the surrounding environmental media (Hasholt *et al.*, 2000).
443 However, the accumulation of contaminated sediments, including remobilised cryoconite, in
444 proglacial lakes, could pose a risk to aquatic ecosystems in some glacial systems, particularly
445 where contaminant levels in supraglacial materials are orders of magnitude higher than those
446 found in Icelandic samples (Owens *et al.*, 2019; Clason *et al.*, 2021).

447

448

449

450

451

452 **Table 5.** Comparison of activity concentrations ranges (Bq kg⁻¹) for ¹³⁷Cs, ²¹⁰Pb and ²⁴¹Am for selected
 453 glaciers in the northern and southern hemispheres.

Glacier and location	Range or mean activity concentrations (Bq kg ⁻¹)			Reference
	¹³⁷ Cs	²¹⁰ Pb	²⁴¹ Am	
Falljökull, Virkisjökull, Skaftafellsjökull, Iceland	1.8 to 169	29.5 to 850	0.6 to 6.1	This study
Adishi Glacier, Georgia	580 to 4,940	1,400 to 12,000	8.1 to 68.3	Łokas <i>et al.</i> (2018)
Morteratsch Glacier, Switzerland	325 to 13558	1581 to 4143	2.9 to 120	Baccolo <i>et al.</i> (2020a)
Ecology Glacier, Antarctica	185 to 350	1400 to 2600	1.69 to 5.02	Buda <i>et al.</i> (2020)
Isfallsglaciären, Sweden	1010 to 4530	5760 to 14700	6.1 to 74	Clason <i>et al.</i> (2021)
Orwell Glacier, Antarctica	0.48 to 54.4	5.5 to 249.1	MDA to 1.61	Owens <i>et al.</i> (2023)

454

455 5. Conclusions

456 This investigation has identified, for the first time, the spatial variability of radioactive and
 457 trace elements in cryoconite samples and glacier mice from Icelandic glaciers. Local geology
 458 and natural particulate sources such as volcanic ash and dust likely contribute to the main
 459 geochemical composition of the Icelandic cryoconite. The radionuclides and many of the trace
 460 elements were higher in cryoconite than the proglacial sediments from the control site. The
 461 activity concentrations are, however, relatively low compared to published values from other
 462 glaciers in the northern hemisphere, and these already low values would likely be further
 463 diluted during transport within the downstream proglacial system. We also reported, for the
 464 first time, the trace element and radioactive content of Icelandic glacier mice, which are a
 465 prominent feature of the Falljökull supraglacial ecosystem. The capacity of glacier mice to
 466 acquire elevated radionuclide activities, in line with those found in cryoconite, suggests they
 467 require further investigation to understand their role in sequestering both radioactive and stable
 468 elements. While the efficient accumulation of radionuclides in both cryoconite and glacier mice

469 is elevated over background values, it is still below levels of contamination that would be likely
470 to pose a risk to the downstream environment in this region. Nevertheless, as a ubiquitous
471 component of the supraglacial ecosystem, cryoconite offers an opportunity to monitor
472 environmental radioactivity in areas where flora typically used for this purpose are rare or
473 absent.

474

475 **Acknowledgements**

476 CCC thanks the Quaternary Research Association for funding that supported fieldwork in
477 Iceland.

478

479 **Author contributions**

480 CCC devised the study, CCC and RF conducted field sampling, ES, GM, CCC and AT
481 conducted sample analysis, and ES, GM and CCC conducted interpretation of the data. All
482 authors contributed to preparation of the manuscript, led by ES.

483

484 **Data availability**

485 Data presented in this manuscript are available within the manuscript and its appendices.

486

487 **References**

488 Arnalds, O., Dagsson-Waldhauserova, P. and Olafsson, H. (2016). The Icelandic volcanic
489 aeolian environment: Processes and impacts- A review, *Aeolian Research*, 20, 176-
490 195.<https://doi.org/10.1016/j.aeolia.2016.004>.

491 Baccolo, G., Di Mauro, B., Massabò, D., Clemenza, M., Nastasi, M., Delmonte, B., Prata, M.,
492 Previtali, E. and Maggi, V. (2017). Cryoconite as a temporary sink for anthropogenic species

493 stored in glaciers, *Scientific Reports*, 7, 9623. <https://doi.org/10.1038/s41598-01-017-10220->
494 5.

495 Baccolo, G., Łokas, E., Gaca, P., Massabò, D., Ambrosini, R., Azzoni, R.S., Clason, C., et al.,
496 (2020a). Cryoconite as an efficient monitor for the deposition of radioactive fallout in glacial
497 environments, *The Cryosphere*, 14, 1-25. <https://doi.org/10.1038/s415598-017-10220-5>.

498 Baccolo, G., Nastasi, M., Massabò, D., Clason, C., Di Mauro, B., Di Stephano, E., Łokas, E.,
499 et al. (2020b). Artificial and natural radionuclides in cryoconite as tracers of supraglacial
500 dynamics: insights the Morteratsch glacier (Swiss Alps). *Catena*, 191, 104577.
501 <https://doi.org/10.1016/j.catena.2020.104577>.

502 Beard, D.B., Clason, C., Rangecroft, S., Poniecka, E., Ward, K.J. and Blake, W.H. (2022).
503 Anthropogenic contaminants in glacial environments 1: Inputs and accumulation. *Progress in*
504 *Physical Geography*, 46, 630-648. <https://doi.org/10.1177/0309/333221107376>.

505 Benediktsson, Í.Ö., Brynjólfsson, S., Ásbjörnsdóttir, L. and Farnsworth, W.R. (2024). Chapter
506 12 – Holocene glacial history and landforms of Iceland, in Palacios, D., Hughes, P.D., Jomelli,
507 V. and Tanarro, L.M. (eds), *European Glacial Landscapes*, 193-224,
508 <https://doi.org/10.1016/B978-0-323-99712-6.00012-X>

509 Buda, J., Łokas, E., Pietryka, M., Richter, D., Magowshi, W., Iakovenko, N., et al. (2020).
510 Biotope and biocenosis of cryoconite hole ecosystems on Ecology Glacier in the maritime
511 Antarctic. *Science of the Total Environment*, 724, 164138112.
512 <https://doi.org/10.1017/j.scitotenv.2020.138112>.

513 CCME (1995). Canadian Council of Ministers of the Environment: Canadian Sediment Quality
514 Guidelines for the protection of aquatic life. CCME EPC-SE. Summary Tables, Environment
515 Canada. Winnipeg, Canada, 1-5.

516 Clason, C., Blake, W.H., Selmes, N., Taylor, A., Boeckx, P., et al. (2021). Accumulation of
517 legacy fallout radionuclides in cryoconite on Isfallsglaciären (Arctic Sweden) and their
518 downstream spatial distribution. *The Cryosphere*, 15, 5151-5168. [https://doi.org/10.5194/tc-](https://doi.org/10.5194/tc-15-5151-2021)
519 15-5151-2021.

520 Clason, C., Baccolo, G., Łokas, E., Blake, W., Owens, P., Cook, et al. (2023a). Global
521 variability and controls on the accumulation of fallout radionuclides in cryoconite. *Science of*
522 *the Total Environment*, 894, 164902. <https://doi.org/10.1016/j.scitotenv.2023.164902>.

523 Clason, C., Rangecroft, S., Owens, P.N., Łokas, E., Baccolo, G., Selmes, N., Beard, D., Kitch,
524 J., Dextre, R.M., Morera, S. and Blake, W. (2023b) Contribution of glaciers to water, energy
525 and food security in mountain regions: current perspectives and future priorities, *Annals of*
526 *Glaciology*, 63(87-89):73-78. <https://doi.org/10.1017/aog.2023.14>

527 Cook, J., Edwards, A., Takeuchi, N. and Irvine-Fynn, T. (2016) Cryoconite: The dark
528 biological secret of the cryosphere, *Progress in Physical Geography*, 40, 66-73.
529 doi:10.1177/030913331566574.

530 Corcho Alvarado, J.A., Steinmann, P., Estier, S., Bochud, F., Haldimann, M. and Froidevaux,
531 P. (2014). Anthropogenic radionuclides in atmospheric air over Switzerland during the last few
532 decades. *Nature Communications* 5, 3030. doi:10.1036/ncomms.1030(2014).

533 Coulson, S.J. and Midgley, N.G. (2012). ‘The role of glacier mice in the invertebrate
534 colonisation of glacial surfaces: the moss balls of the Falljökull, Iceland’, *Polar Biology*, 35,
535 1651-1658. doi: 10.1007/s00300-012-1205-4.

536 Davidson, H., Millward, G.E., Clason, C.C., Fisher, A., Taylor, A. (2023). Chemical
537 availability of fallout radionuclides in cryoconite. *Journal of Environmental Radioactivity*,
538 268-269, 107260. <https://doi.org/10.1016/j.envrad.2023.107260>.

539 Denk, T., Grimsson, F., Zetter, R. and Simonarson, L.A. (2011). Introduction to the Nature and
540 Geology of Iceland in: Denk, T., Grimsson, F., Zetter, R. and Simonarson, L.A. *Late Cainozoic*
541 *Floras of Iceland*. Dordrecht: Springer, 1-29.

542 Einarsson, M.Á. (1984). ‘Climate of Iceland’ in van Loon, H. (eds) *Climates of the Oceans*.
543 Amsterdam: Elsevier, pp. 673–697.

544 Evans, D.J.A., Ewertowski, M. and Ortona, C. (2017). Skaftafellsjökull, Iceland: glacial
545 geomorphology recording glacier recession since the Little Ice Age. *Journal of Maps*, 13, 358-
546 368. <https://doi.org/10.1080/17445647.2017.1310676>.

547 Everest, J., Bradwell, T., Jones, L. and Hughes, L. (2017). The geomorphology of
548 Svínafellsjökull and Virkisjökull-Falljökull glacier forelands, southeast Iceland’, *Journal of*
549 *Maps*, 13, 936-945. <https://doi.org/10.1080/17445647.2017.1407272>.

550 Hannesdóttir, H., Zöhrer, A., Davids, H., Sigurgeirsdóttir, S., Skimisdóttir and Ámason, P.
551 (2013) *Vatnajökull National Park: Geology and Geodynamics*. Available on line at:
552 [https://www.uef.fi/documents/640649/725289/NEED+V_New+Geo+Review.pdf/273c6abe-](https://www.uef.fi/documents/640649/725289/NEED+V_New+Geo+Review.pdf/273c6abe-c105-4c36-83cb-a5cc3fdaf930)
553 [c105-4c36-83cb-a5cc3fdaf930](https://www.uef.fi/documents/640649/725289/NEED+V_New+Geo+Review.pdf/273c6abe-c105-4c36-83cb-a5cc3fdaf930). (Accessed 11 March 2020)

554 Hasholt, B., Walling, D.E. and Owens, P.N. (2000). Sedimentation in Arctic proglacial lakes,
555 Mittivakkat Glacier, south east Greenland, *Hydrological Processes*, 14, 679-699. doi:
556 10.1002/(SICI)1099.1085(2000003)14:4<679::AID-HYP966>3.0.CO;2-E

557 He, L., Wang, S., Liu, M., Chen, Z., Xu, J. and Dong, Y. (2023) Transport and transformation
558 of atmospheric metals in ecosystems: A review, *Journal of Hazardous Materials Advances*, 9,
559 100218, <https://doi.org/10.1016/j.hazadv.2022.100218>

560 Hotaling, S., Bartholomaus, T.C. and Gilbery, S.L. (2020). Rolling stones gather moss:
561 movement and longevity of moss balls on an Alaskan glacier, *Polar Biology*, 43, 735-744.
562 <https://doi.org/10.1007/s00300-020-02675-6>

563 Łokas, E., Zaborska, A., Kolicka, M., Różycki, M. and Zawierucha, K. (2016). Accumulation
564 of atmospheric radionuclides and heavy metals in cryoconite holes on an Arctic glacier,
565 *Chemosphere*, 160, 162-172. <http://dx.doi.org/10.1016/j.chemosphere.2016.06.051>.

566 Łokas, E., Wachniew, P. Jodłowski, P. and Gąsiorek, M. (2017) Airborne radionuclides in the
567 proglacial environment as indicators of sources and transfers of soil material, *Journal of*
568 *Environmental Radioactivity*, 178-179, pp. 193-202.
569 <https://doi.org/10.1016/j.envrad.2017.08.018>.

570 Łokas, E., Zawierucha, K., Cwanek, A., Szufa, K., Gaca, P., Mietelski, J.W. and
571 Tomankiewicz, E. (2018) The sources of high airborne radioactivity in cryoconite holes from
572 the Caucasus (Georgia), *Scientific Reports*, 8:10802. doi:10.1038/s41598-018-29076-4.

573 Łokas, E., Zaborska, A., Sobota, I., Gaca, P., Milton, J.A., Kocurek, P. and Cwanek, A. (2019)
574 Airborne radionuclides and heavy metals in high Arctic terrestrial environment as the
575 indicators of sources and transfers of contamination, *The Cryosphere*, 13, 2075-2086.
576 doi.org/10.5194/tc-2019.34.

577 Łokas, E., Wachniew, P. Baccolo, G., Gaca, P., Janko, K. Milton, A., et al. (2022). Unveiling
578 the extreme environmental radioactivity of cryoconite from a Norwegian glacier. *Science of*
579 *the Total Environment*, 814, 152656. <http://dx.doi.org/10.1016/j.scitotenv.2021.152656>.

580 Lutz, S., Anesio, A.M., Edwards, A. and Benning, L.G. (2015) Microbial diversity on Icelandic
581 glaciers and ice caps, *Frontiers in Microbiology*, 6 (307), pp. 1-17.
582 <https://doi.org/10.3389/fmicb.2015.00307>.

583 Meinander, O., Dagsson-Waldhauserova, P., Arnalds, O. (2016). Icelandic volcanic dust can
584 have a significant influence on the cryosphere in Greenland and elsewhere. *Polar Research*,
585 35, 31313. <https://doi.org/10.3422/polar.v35.31313>.

586 Ministry of Environment, Iceland (2006). *Iceland's National Programme of Action for the*
587 *Protection of the Marine Environment from Land-Based Activities*. Available at:
588 https://www.government.is/media/umhverfissraduneyti-media/media/PDF_skrar/GPA.pdf
589 (Accessed 03 March 2020).

590 Nagatsuka, N., Takeuchi, N., Uetake, J., Shimada, R. (2014). Mineralogical composition of
591 cryoconite on glaciers in northwest Greenland. *Bulletin of Glaciological Research*, 32, 107-
592 114. doi:10.5331/bgr.32.107.

593 Owens, P.N., Blake, W.H. and Millward, G.E. (2019) Extreme levels of fallout radionuclides
594 and other contaminants in glacial sediment (cryoconite) and implications for downstream
595 aquatic ecosystems, *Scientific Reports*, 9, 1-9. <https://doi.org/10.1038/s41598-019-48873-z>.

596 Owens, P.N., Stott, T.A., Blake, W.H. and Millward, G.E. (2023) Legacy radionuclides in
597 cryoconite and proglacial sediments on Orwell Glacier, Signy Island, Antarctica. *Journal of*
598 *Environmental Radioactivity*, 264, 107206. <https://doi.org/10.1038/s41598-019-48873-z>.

599 Pálsson, S.E., Arnalds, O., Sigurgeirsson, M.A., Guonason, J., Howard, B.J., Wright, S.M. and
600 Pálsdóttir, P. (2002) Cs-137 fallout inventories in Iceland - estimating deposition from
601 precipitation data, *Radioprotection*, 37(C1), 1223-1228,
602 <https://doi.org/10.1051/radiopro/2002151>

603 Phillips, E., Finlayson, A., Bradwell, T., Everest, J. and Jones, L. (2014) Structural evolution
604 triggers a dynamic reduction in active glacier length during rapid retreat: Evidence from

605 Falljökull, SE Iceland, *Journal of Geophysical Research: Earth Surface*, 119, 2194-2208.
606 <https://doi.org/10.1002/2014JF003165>.

607 Rozwalak, P., Podkowa, P., Buda, J., Niedzielski, P., Kawecki, S', Ambrosini, R., et al.,
608 (2022). Cryoconite – from minerals and organic matter to bioengineered sediments on glacier's
609 surfaces. *Science of the Total Environment*, 807, 150874.
610 <https://doi.org/10.1016/j.scitotenv.2021.150874>.

611 Rudnick, R.L. and Gao, S. (2014) Composition of the Continental Crust, *Treatise on*
612 *Geochemistry 2nd edition*, 3, 1-51. doi:10.1016/B0-08-043751-6/03016-4.

613 Singh, S.M., Sharma, J., Gawas-Sakhalkar, P., Upadhyay, A.K., Naik, S., Pedneker, S.M. and
614 Ravindra, R. (2013) Atmospheric deposition studies of heavy metals in Arctic by comparative
615 analysis of lichens and cryoconite, *Environmental Monitoring and Assessment*, 185, 1367–
616 1376. <https://doi.org/10.1007/s10661-012-2638-5>.

617 Steinhauser, G., Brandl, A., and Johnson, T.R. (2014). Comparison of the Chernobyl and
618 Fukushima nuclear accidents: a review of the environmental impacts. *Science of the Total*
619 *Environment*, 470-471,800-817. <https://doi.org/10.1016/j.scitotenv.2013.10.029>.

620 Takeuchi, N. (2002). Optical characteristics of cryoconite (surface dust) on glaciers: the
621 relationship between light absorbency and the property of organic matter contained in the
622 cryoconite, *Annals of Glaciology*, 34, 409-414, doi:10.3189/172756402781817743

623 UNSCEAR. 2000. *Sources And Effects Of Ionizing Radiation*. United Nations Publications,
624 New York.

625 Vilmundardóttir, O.K., Gísladóttira, G. and Lala, R. (2014) Early stage development of
626 selected soil properties along the proglacial moraines of Skaftafellsjökull glacier, SE-Iceland,
627 *Catena*, 121, pp. 142-150. doi: 10.1016/j.catena.2014.04.020.

628 Vogel, A., Diplas, s., Durant, A.J., Azar, A.S., Sunding, M.F., Rose, W.I, Sychkova, A. et al.
629 (2016). Reference dataset of volcanic ash physiochemical and optical properties. *Journal of*
630 *Geophysical Researc: Atmospheres*, 122, 9485-9514. <https://doi.org/10.1002/2016JD026328>.

631 Wejnerowski, Ł., Poniecka, E., Buda, J., Klimaszyk, P., Piasecka, A., Dziuba, M.K., Mugnai,
632 G., Takeuchi, N. and Zawierucha, K. (2023), Empirical testing of cryoconite granulation: Role
633 of cyanobacteria in the formation of key biogenic structure darkening glaciers in polar regions,
634 *Journal of Phycology*, 59(5), 939-949, <https://doi.org/10.1111/jpy.13372>

635 Wilflinger, T., Lettner, H., Hubmer, A., Bossew, P., Sattler, B. and Slupetzky, H. (2018)
636 Cryoconites from Alpine glaciers: Radionuclide accumulation and age estimation with Pu and
637 Cs isotopes Pb-210, *Journal of Environmental Radioactivity*, 186, 90-100.
638 <https://doi.org/10.1016/j.envrad.2017.06.020>.

639 Zawierucha, K., Buda, J., Pietryka, M., Richter, D., Łokas, E., Lehmann-Konera, S., Makoska,
640 N. and Bogdziewicz, M. (2018) Snapshot of micro-animals and associated biotic and abiotic
641 environmental variables on the edge of the south west Greenland ice sheet, *Limnology*, 19, 141-
642 150. <https://doi.org/10.1007/s10452-019-09681-9>.